Eur. Phys. J. B **53**, 35–38 (2006)
DOI: 10.1140/epjb/e2006-00350-3

THE EUROPEAN PHYSICAL JOURNAL B

Electronic properties of multi-quantum dot structures in $Cd_{1-x}Zn_xS$ alloy semiconductors

N. Safta[1,a], A. Sakly[2], H. Mejri[1,3], and M.A. Zaïdi[1]

[1] Laboratoire de Physique des Semi-conducteurs et des Composants Électroniques, Faculté des Sciences, Avenue de l'environnement, 5000 Monastir, Tunisia
[2] Unité de Physique Quantique, Faculté des Sciences, Avenue de l'environnement, 5000 Monastir, Tunisia
[3] École Préparatoire aux Académies Militaires, Avenue Maréchal Tito, 4029 Sousse, Tunisia

Received 6 March 2006 / Received in final form 23 May 2006
Published online 22 September 2006 –

Abstract. In this paper, we present a theoretical study of the quantized electronic states in $Cd_{1-x}Zn_xS$ quantum dots. The shape of the confining potential, the subband energies and their eigen envelope wave functions are calculated by solving a one-dimensional Schrödinger equation. Electrons and holes are assumed to be confined in dots having a flattened cylindrical geometry with a finite barrier height at the boundary. Optical absorption measurements are used to fit the bandgap edge of the $Cd_{1-x}Zn_xS$ nanocrystals. An analysis of the electron band parameters has been made as a function of Zn composition. Two main features were revealed: (i) a multiplicity in $Cd_{1-x}Zn_xS$ quantum dots with different crystalline sizes has been found to fit accurately experimental data in the composition range $0 \leq x \leq 0.2$; (ii) the fit did not, however, show a multiplicity for x higher than 0.4. On the other hand, we have calculated the energy level structure of coupled $Cd_{1-x}Zn_xS$ semiconductor quantum dots using the tight-binding approximation. As is found the Zn composition $x = 0.4$ is expected to be the most favorable to give rise a superlattice behavior for the $Cd_{1-x}Zn_xS$ quantum dots studied.

PACS. 73.21.La Quantum dots – 73.22.-f Electronic structure of nanoscale materials: clusters, nanoparticles, nanotubes, and nanocrystals – 71.55.Gs II-VI semiconductors

1 Introduction

From the fundamental view point, the study of electronic and optical properties of quantum dots (QD's) in III–V and II–VI nanostructures is attracting a considerable interest [1–15]. They also present various practical applications [8,12,16–21]. Concerning the QD's based on II–VI semiconductors, less studied, is the $Cd_{1-x}Zn_xS$ system, despite the high potentiality of this material in device design as an essential compound in solar cells [16,17,22,23]. Theoretically, as for the other II–VI QD's, the electronic properties of $Cd_{1-x}Zn_xS$ nanoparticles have been usually investigated using a spherical geometry model with an infinite potential barrier at the boundary [8–12]. As was found, this model evidences the quantum confinement in $Cd_{1-x}Zn_xS$ nanocrystals. It can not, however, account for the coupling between QD's. In a recent study, we have investigated the electronic properties of $Cd_{1-x}Zn_xS$ nanocrystals [13]. We adopted the spherical geometry model, but with finite potential barriers. Both electrons and holes are assumed to be confined in nanospheres. Using this model, we have calculated the shape of the confining potential, the quantized energies as well as the exciton bound states and the oscillator strength of interband transitions. This approach has an advantage to access to unknown fundamental parameters of $Cd_{1-x}Zn_xS$ QD's such as the crystallite size and the barrier potential heights. Nevertheless, the spherical geometry model does not lend simply to a computation of the band edges for coupled QD's, namely along different quantization directions.

For III–V semiconductors, several works have attempted to determine the geometry of QS's [1–7]. These investigations have failed to provide details on the shape and crystalline size. In addition, the QD sizes were usually used as adjustable parameters to fit experimental data. Williamson et al suppose that QD's can have a lens and pyramidal shapes [6]. They also considered different geometries including these two shapes. Grundmann et al have evoked three types of elementary structures, the pseudomorphic slab, cylinder and sphere to calculate the strain distribution in and around pyramidal InAs/GaAs QD's [7]. Based on these works and for sake of simplicity, we adopted the flattened cylindrical geometry in describing the $Cd_{1-x}Zn_xS$ nanoparticles.

The present work reports on the modeling of $Cd_{1-x}Zn_xS$ QD's with the aim to investigate their confinement properties. Our interest has been focused, in

[a] e-mail: saftanabil@yahoo.fr

Table 1. Parameters used to calculate the electronic states of $Cd_{1-x}Zn_xS$ QD's. Also reported in the table are the relevant confinement energies ε_e and ε_h, E_g^{eff} and E_g^{bulk} versus Zn composition.

x	$\frac{m_e^*}{m_0}$	$\frac{m_h^*}{m_0}$	V_e (eV)	V_h (eV)	L (nm)	ε_e (eV)	ε_h (eV)	E_g^{bulk} (eV)	E_g^{eff} (eV)
0.0	0.16	5.00	0.10	0.25	1.0	0.090	0.040	2.42	2.56
			0.25	0.10	2.0	0.133	0.011		
			1.00	0.10	3.0	0.146	0.005		
0.2			0.25	0.25	1.0	0.195	0.044	2.61	2.85
			1.00	0.10	2.0	0.233	0.012		
0.4			0.45	0.50	1.0	0.280	0.060	2.82	3.16
0.6			0.75	0.50	1.0	0.386	0.069	3.05	3.51
0.8			1.50	0.50	1.0	0.490	0.083	3.31	3.89
1.0	0.28	1.76	2.00	2.00	1.0	0.557	0.145	3.60	4.30

particular, on the coupling between QD's. For this purpose, we have considered the $Cd_{1-x}Zn_xS$ nanocrystallites having a flattened cylindrical geometry with a finite potential barrier at the boundary. Calculations have been carried out versus Zn composition going from CdS to ZnS. After an introduction, we report an outline on the computational method. Discussion of results and conclusions are presented in the following.

2 Modeling and results

The system to simulate consists of an electron and a hole, both being confined in a $Cd_{1-x}Zn_xS$ QD. The latter is assumed to having a cylindrical geometry of radius R and a height L. The semiconductor material is capped inside a dielectric host matrix. According to that reported in reference [6], lens-shaped QD's have as circular base with diameter 25 nm and a height of 3.5 nm; while those of pyramidal forms have a diameter of 11.3 nm and a height of 5.6 nm respectively. If, similarly, the QD's being studied have a diameter larger than the height, ie they show a flattened cylindrical geometry, the quantum confinement along the transversal directions of the cylinder can be disregarded. Using this approximation, the problem to solve reduces to that of a one-dimensional potential. Hence, the electron and hole states in a QD are given from the Hamiltonian:

$$H = -\frac{\hbar^2}{2m_{e,h}^*}\frac{d^2}{dz_{e,h}^2} + V_{e,h}\left(z_{e,h}\right) \qquad (1)$$

where $\hbar$ is the Plank's constant, m^* is the effective mass of free carriers, z is the direction perpendicular to the QD base and $V(z)$ represents the potential energy. The subscripts e and h refer to the electron and hole particles respectively. Based on the flattened cylindrical geometry assumption, $V(z)$ can be modeled by a square-shaped potential with a width L and a barrier height V. In deriving the Hamiltonian H, we have adopted the effective mass theory (EMT) and the band parabolicity approximation (BPA) as well. The mismatch of the effective mass between the well and the barrier has been neglected. Values of the electron and hole effective masses, as calculated for CdS and ZnS [24], are listed in Table 1. These two parameters for $Cd_{1-x}Zn_xS$ dots with different Zn compositions have been deduced using the Vegard's law. In solving the single-particle Schrödinger equation for electrons and holes, V_e, V_h and L were treated as fitting parameters. Using equation (1), we have computed the confinement energies of free carriers, ε_e and ε_h, versus Zn composition. The results obtained are summarized in Table 1. The characteristic V_e, V_h and L parameters for $Cd_{1-x}Zn_xS$ QD's investigated were derived as follows: $\varepsilon_e+\varepsilon_h = E_g^{eff} - E_g^{bulk}$, where E_g^{eff} is the effective band gap of $Cd_{1-x}Zn_xS$ QD's and E_g^{bulk} is the band gap energy of bulk $Cd_{1-x}Zn_xS$. Values of E_g^{eff} are deduced from absorption measurements, performed on sol-gel grown $Cd_{1-x}Zn_xS$ nanocrystals [12]. As for the x-dependence of E_g^{bulk}, it is taken from reference [23]. It is worth noticing that the sum of ε_e and ε_h corresponds to the band gap widening, which is induced by a confinement effect. As is found from this study, calculations reveal a multiplicity of three types of QD's for CdS, which differ in crystallite size L and in the barrier heights V_e and V_h. Also shown in the table is the increasing of V_e with L. Whereas the potential barrier V_h for holes shows a decreasing tendency as L increases. As for the confinement energies, ε_e and ε_h vary in inverse proportion so as their sum keeps the same bandgap widening $\Delta E_g\,(x=0) = 0.14$ eV. For $Cd_{1-x}Zn_xS$ with $x = 0.2$, we have distinguished only two types of QD's, associated with $L = 1$ and 2 nm. It should be noted that the electron band parameters V_e, V_h, ε_e and ε_h show the same trend versus L compared to that of CdS. In the case of $Cd_{1-x}Zn_xS$ nanocrystallites having a Zn molar fraction larger than 0.4, the absorption results were fitted accurately by using a single distribution of QD's. The latter is characterized by a crystalline size L of 1 nm. The hole confinement energy is not, however, large for $Cd_{1-x}Zn_xS$ QD's independently of their compositions. The reasons of this are: firstly the Cd substitution by a Zn atom induces a potential more attractive for the electrons, secondly there is a large difference between the electron and hole effective masses in CdS, ZnS and in their alloys.

An attempt to explain the multiplicity of $Cd_{1-x}Zn_xS$ QD's is as follows. For CdS ($x = 0$), the crystal structure is typically hexagonal. While, for higher Zn contents, the

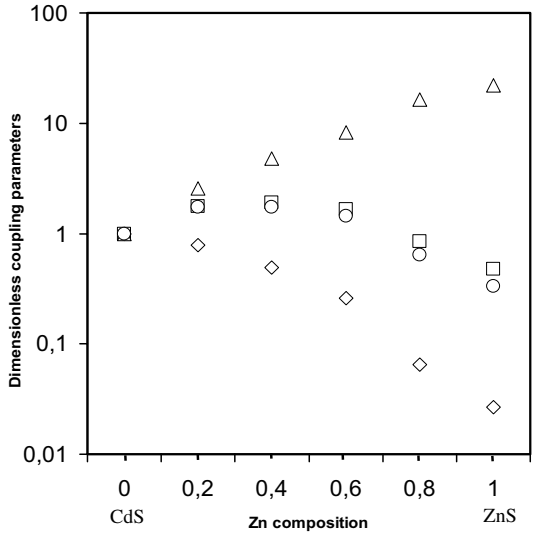

Fig. 1. Normalized coupling integrals versus x for $Cd_{1-x}Zn_xS$ QD's: $\Diamond$ $r_{e,e}(x)/r_{e,e}(0)$; $\square$ $\beta_e(x)/\beta_e(0)$; $\triangle$ $\gamma_e(x)/\gamma_e(0)$; $\circ$ $\Delta E_e(x)/\Delta E_e(0)$. Values of $r_{e,e}$, β_e, γ_e and ΔE_e for $x = 0$ are 0.93, 0.080 eV, 0.090 eV, 0.069 eV respectively.

latter changes from wurtzite to cubic [26–30]. Therefore, a phase transition in the crystal structure of $Cd_{1-x}Zn_xS$ occurs at an intermediate Zn composition x. Values of this composition, as reported in different works, range from 0.27 to 0.80 [27–30]. As is also known, the crystalline sizes of the $Cd_{1-x}Zn_xS$ ternary alloy show a decreasing trend with increased Zn compositions. For these reasons, in the case of low Zn compositions, the nucleation of hexagonal elementary cells can give rise to a variety of QD's, which differ in the crystallite size. However, for higher ZnS molar fractions, the assembling of elementary cells in cubic phase preserves the uniformity in geometry, which leads to a single distribution of QD's. The latter ones are characterized by the same crystallite size.

In designing semiconductor devices, a crucial problem to solve is to accelerate processes governing the transfer of carriers. The ways of reducing the switching time are to shorten the carrier transfer distance and increase the carriers' velocity. High electron mobility transistors having a two-dimensional electron gas created in an extremely short channel were realized using this procedure. Another approach is to use nanostructures containing tunneling-coupled QD's as an active element. Let us now consider the electron-hole pair in a double quantum dot (DQD). The dots are assumed to be cylindrical. The ground state of this system can be described simply if the electron-hole interaction is neglected. For the DQD considered, one has to add the potential $V_{eh}(z_{eh} - d)$ with d being the spatial separation of QD's to the Hamiltonian of equation (1). By solving the total Hamiltonian with use the tight banding approximation (TBA), we have calculated the wave function overlap, the exchange and the correlation integrals as well as the energy levels' splitting versus Zn composition. We have denoted them by r, β, γ and ΔE respectively. Calculations were carried out for $d = 2$ nm. The results are depicted in Figure 1. As can be noticed from the plots, the electron wave function overlap $r_{e,e}$ decreases with increased x. Both β_e and ΔE_e are shown to increase with Zn composition up to $x = 0.4$ and they decrease in the same way as x increases from 0.4 to 1.0. As for γ_e, this parameter, however, shows an increasing tendency with x. The latter study led to three main observations: (i) for $Cd_{1-x}Zn_xS$ QD's with a low zinc content, the interaction between electron gases is mainly induced by the wave function overlap and exchange effects; (ii) for the intermediate composition $x = 0.4$, the coupling between QD's is the highest for which the energy splitting ΔE is maximum; (iii) at high zinc compositions, the electron coupling is ensured by correlation effects rather than the overlap and the exchange; the nanocrystallites, however, tend to behave as isolated QD's. As well demonstrated from this study, $Cd_{1-x}Zn_xS$ QD's with Zn composition close to $x = 0.4$ are appropriate to form superlattice structures for electrons. For the holes, the same trend has been observed for the r, β, γ and ΔE parameters as a function of x. Except that these parameters remain insignificant, which means that the strong localization character of holes in the QD's is highly preserved going from CdS to ZnS.

3 Conclusion

We investigated at first the electronic properties of single $Cd_{1-x}Zn_xS$ QD's for Zn composition ranging from CdS to ZnS. To describe the QD's, we have considered a flattened cylindrical geometry with a finite potential barrier at the boundary. Using the model of a square-shaped potential, we have calculated the band edges of $Cd_{1-x}Zn_xS$ QD's as a function of composition x. As an experimental support, we have used absorption data, obtained on $Cd_{1-x}Zn_xS$ nanocrystalline thin films prepared by the sol-gel technique. An analysis of the results has evidenced a multiplicity in QD's with different crystallite sizes at low Zn compositions only. On the other hand, we have studied the electronic properties of coupled $Cd_{1-x}Zn_xS$ QD's. Based on the TBA, we have computed the coupling parameters such as the wave function overlap, the exchange and correlation integrals as well as the splitting of the ground states versus Zn composition. As has been demonstrated from the latter study, $Cd_{1-x}Zn_xS$ QD's with composition x close to 0.4 can exhibit a superlattice behavior for conduction electrons. This can open a way to $Cd_{1-x}Zn_xS$ for designing a new class of QDs' devices.

References

1. W. Yang, H. Lee, P. Sercel, A. Norman, SPIE Photonics **1**, 3325 (1999)
2. W. Yang, H. Lee, J. Johnson, P. Sercel, A. Norman, Phys. Rev. B
3. T. Metzger, I. Kegel, R. Paniago, J. Peisel (private communication, 1999)
4. J. Garcia, G. Medeiros-Ribeiro, K. Scmidt, T. Ngo, F. Feng, A. Lorke, J. Kotthaus, P. Petroff, Appl. Phys. Lett. **71**, 2014 (1997)

5. M. Rubin, G. Medeiros-Ribeiro, J. O'Shea, M. Chin, E. Lee, P. Petroff, V. Narayanamurti, Phys. Rev. Lett. **77**, 5268 (1996)
6. A.J. Williamson, L.W. Wang, A. Zunger, Phys. Rev. B **62**, 19, 12963 (2000)
7. M. Grundmann, O. Stier, D. Bimberg, Phys. Rev. B **52**, 16, 11969 (1995)
8. K.K. Nanda, S.N. Sarangi, S. Mohanty, S.N. Sahu, Thin Solid Films **322**, 21 (1998)
9. Q. Pang, B.C. Guo, C.L. Yang, S.H. Yang, M.L. Gong, W.K. Ge, J.N. Wang, J. Crystal Growth **269**, 213 (2004)
10. M.C. Klein, F. Hache, D. Ricard, C. Flytzanis, Phys. Rev. B **42**, 11123 (1990)
11. H. Yükseici, P.D. Persans, T.M. Hayes, Phys. Rev. B **52**, 16, 11763 (1995)
12. B. Bhattacharjee, S.K. Mandal, K. Chakrabarti, D. Ganguli, S. Chaudhui, J. Phys. D: Appl. Phys. **35**, 2636 (2002)
13. N. Safta, A. Sakly, H. Mejri, Y. Bouazra, Eur. Phys. J. B **51**, 75 (2006)
14. A. Franceschetti, H. Fu, L.W. Wang, A. Zunger, Phys. Rev. B **60**, 1819 (1999)
15. M.C. Troparevsky, L. Kronic, J.R. Chelikowsky, J. Chem. Phys. **119**, 2284 (2003)
16. H.L. Kwok, J. Phys. D/Appl. Phys. **16**, 2367 (1983)
17. K.A. Pal, A. Dhar, A. Mondal, R.L. Basak, S. Chaudhuri, *Proc. IEEE, Las Vegas, Nevada*, 1646 (1988)
18. U. Sohlimg, G. Jung, M. Mennig, J. Sol. Gel Sci. Technol. **13**, 635 (1998)
19. K. Sooklal, B.S. Cullum, S.M. Angel, C.J. Murphy, J. Phys. Chem. **100**, 4551 (1996)
20. P. Reiss, J. Bleuse, A. Pron, Nano Lett. **2**, 781 (2002)
21. P. Reiss, J. Bleuse, F. Chandezon, A. Pron, H. Ulmer-Tuffigo, DRF News. **2**, 10 (2002)
22. V. Alberts, R. Herberhonz, T. Walter, H.W. Schock, J. Phys. D: Appl. Phys. **30**, 2156 (1997)
23. N. Kohara, T. Negami, M. Nishitani, T. Wada, Jpn J. Appl. Phys. **34**, L 1141 (1995)
24. W. Ekardt, K. Losch, D. Bimberg, Phys. Rev. B **20**, 3303 (1979)
25. G.K. Padam, G.L. Mahotra, S.U.M. Rao, J. Appl. Phys. **63**, 770 (1988)
26. G.K. Padam, G.L. Malhotra, S.U.M. Rao, J. Appl. Phys. **63**, 770 (1988)
27. R.L. Basak, S. Chaudhuri, A.K. Pal, J. Mater. Sci. Lett. **7**, 1048 (1988)
28. A. Dhar, R.L. Basak, S. Chaudhuri, A.K. Pal, Indian J. Phys. **64** A, 10 (1990)
29. A. Dhar, S. Chaudhuri, A.K. Pal, J. Mater. Sci. **26**, 4416 (1991)
30. M.W. Kane, J.P. Spratt, L.W. Hershinger, I.M. Khan, J. Electrochem. Soc. **113**, 136 (1966)